ACS OMEGA

http://pubs.acs.org/journal/acsodf

Article

Betanidin pK_a Prediction Using DFT Methods

Sergio A. Rodriguez* and Maria T. Baumgartner

Cite This: https://dx.doi.org/10.1021/acsomega.0c00904

Read Online

ACCESS | Metrics & More | Article Recommendations | Supporting Information

ABSTRACT: Betalains can be used in food, drugs, and cosmetic industries and have shown their bioactive potential. These properties are strongly influenced by pH and other physicochemical conditions. The pK_a values for the polyprotic Betanidin (**Bd**) molecule are unknown, and they are crucial to elucidate the oxidation mechanism in which its pigment is involved. In the present study, the values of pK_a for all protic groups of **Bd** were analyzed using five hybrid density functionals (B3LYP, B3PW91, ωB97XD, PBE0, and M06-2X), five basis sets (6-31+G(d), 6-31+G(d,p), 6-31++G(d,p), 6-311+G(d,p), and 6-311++G(d,p)) and the solvation model based on density (SMD) implicit solvation model. Moreover, one and three explicit water molecules were added to improve the solvation free energy values. Furthermore, the values of pK_a of betanin, betalamic acid, and *cyclo*-dihydroxyphenylalanine (DOPA) were studied. Based on these analyses, we propose the acid−base behavior of **Bd** in water and develop new tools to understand their chemical reactivity.

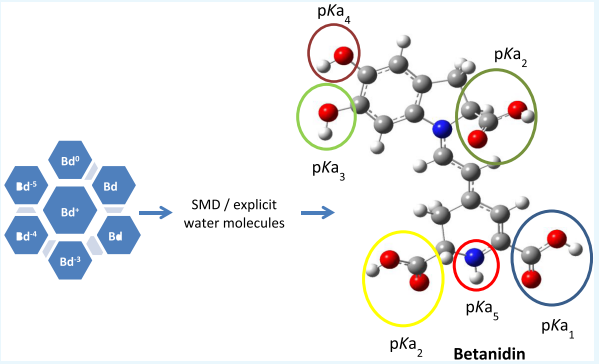

1. INTRODUCTION

Betalains are water-soluble nitrogenous pigments found in high amounts in plant species from the order Caryophyllales.[1] Betalains are divided into two subclasses: betaxanthins (yellow-orange pigments) and betacyanins (red-violet pigments).[2] Betacyanins are derivatives of Betanidin (**Bd**), an iminium compound derived from betalamic acid and *cyclo*-dihydroxyphenylalanine (DOPA), whereas betaxanthins are obtained from the reaction of amines or α-amino acids with betalamic acid, for example, indicaxanthin (**In**) in prickly pear (*Opuntia ficus-indica*).[2] Typically, betalains show good solubility in water and alcohols.[3] Betalains in aqueous solutions are stable in the pH range from 3.5 to 7;[4,5] however, light, metal cations, high temperature, and oxygen reduce the dye stability.[6]

Betalain pigment can be used in food, drugs, and cosmetic industries as beet powder or beet juice concentrate.[7] In recent years, betalains have shown their biological potential; they have antimicrobial, antiviral, and antitumoral effects and anti-inflammatory activity.[8] In addition, the pure natural betalains and semisynthetic analogues have demonstrated to significant reduce of lipoxygenase and cyclooxygenase activity.[9] The strong free radical scavenging capacity and antioxidant activity of these pigments and their modulation by different structural factors have been well documented.[1,10] Moreover, the influence of pH and other physicochemical conditions on the antioxidant activity of betalains has been observed.[10,11]

Betanin (**Bn**, E-number E162), the only betalain approved for use in food and almost mainly obtained from red beet crops,[12] is one of the best-known betacyanin dyes found in a few plants from the Caryophyllales family.[5] Structurally, **Bn** is composed for **Bd**, linked β-glycosidic with glucose at C5. The presence of **Bn** in roots, stems, fruits, leaves, and flower petals results in a characteristic red/purple color.

Temperature is the main factor causing **Bn** decomposition, and light-induced decay at low temperatures may also be important.[13] Molecular oxygen is involved in **Bn** photodegradation, being undetectable in anaerobic conditions. Dehydrogenated and decarboxylated betanins were the main products formed in aqueous solutions upon UV irradiation.[14]

On the other hand, **Bd** was exposed to oxidation by enzyme tyrosinase, a polyphenol oxidase that plays a key role in the betalain biosynthetic scheme.[15] Moreover, the same oxidation products profile of betalains by peroxidase enzyme was reported.[16] Recently, the enzymatic oxidation of **Bd** and **Bn**, followed by chromatographic separation of the oxidation products with spectrophotometric and mass spectrometric detection (LC-DAD-MS/MS) was studied.[17] In that article, dehydrogenated, decarboxylated, and *o*-quinone oxidation products were identified, and their proportions were closely related to the average medium pH. Besides, the oxidation mechanism was proposed from the fully protonated betalain. Similar results were reported for the electrochemical oxidation of **Bd**.[18] The chemical oxidation of **Bn** by 2,2′-azinobis(3-

Received: February 28, 2020
Accepted: May 22, 2020

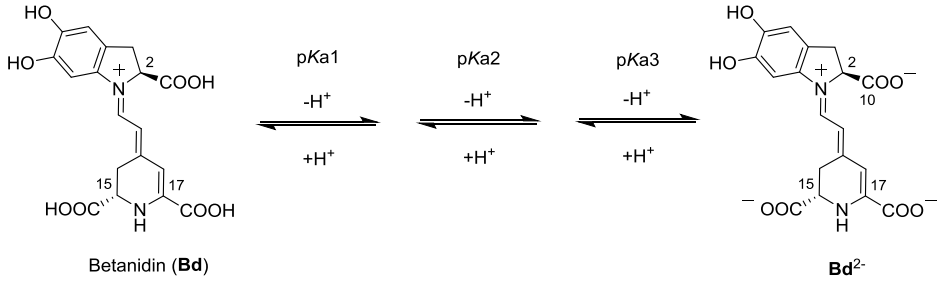

Figure 1. Carboxylic deprotonation steps of **Bd**.

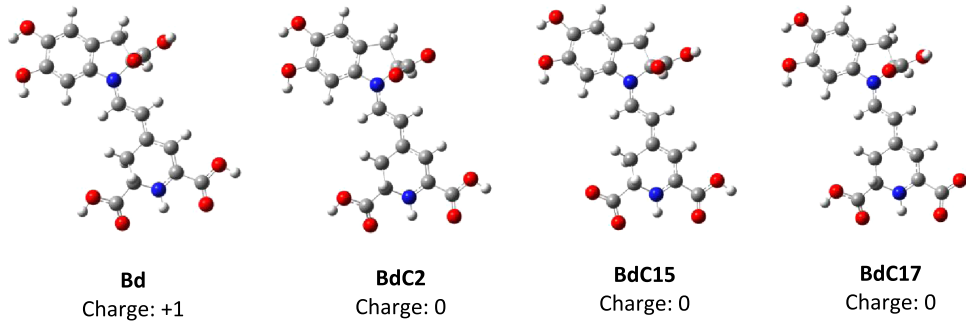

Figure 2. B3LYP/6-31+G(d) optimized structures of mono-deprotonated **Bd** in the three carboxylic positions using the SMD implicit solvent model.

ethylbenzthiazoline-6-sulfonic acid) (ABTS) radical also resulted in the formation of dehydrogenated and decarboxylated derivatives, presumably followed by a one-electron oxidation product as an intermediate.[19]

On the other hand, the same product's profile was found by the thermal treatment of betalains in aqueous and alcoholic media.[6] Moreover, these compounds were identified as products from **Bn** oxidation catalyzed by Cu^{2+} cations in aqueous solutions at neutral pH, but an alternative mechanism was proposed.[20] Besides, the oxidation of the excited **Bn** was studied using electrochemistry techniques and a two-electron oxidation mechanism was proposed without conclusive evidence.[21,22]

Despite the potential of betalains and based on the above discussion, it is clear that systematic research on their oxidation mechanism is still insufficient, particularly the study of pH incidences on the oxidation pathways. Acid dissociation constant (pK_a) is essential for evaluating the acid−base properties of betalains, but they remain unknown. Direct measurement of the pK_a values with traditional experimental approaches for each functional group involving complex aqueous samples can be defying. Thus, the accurate calculation of the values of pK_a with theoretical methods is very interesting. An extensively used method for calculating the values of pK_a implies the use of quantum chemical calculations, typically density functional theory (DFT), and the solvation model based on density (SMD), as an electron density-based solvation model.[23,24]

Many methodologies have been used to calculate the values of pK_a with computational chemistry approaches. One of the most common methods involves the use of an appropriate thermodynamic cycle to calculate the aqueous Gibbs free energy of deprotonation.[25] Another ever more common methodology is the "direct" approach, where the geometries are optimized and deprotonation free energies calculated directly in the presence of the continuum solvent without the necessity for gas-phase calculations. A succession of studies comparing methods using thermodynamic cycles and the direct approach showed that the two approaches can accomplish comparable accuracy.[23,24] On the other hand, including first-shell explicit water molecules, is an additional tool to enhance the accuracy of pK_a calculations. Using this methodology, it was proved that including explicit water molecules as hydrogen bond donors or acceptors to dicarboxylic acids reduced the error in calculations compared continuum solvation alone.[26]

In the present study, the values of pK_a for all protic groups of **Bd** were analyzed using many computational approaches to unveil its acid−base behavior and develop new tools to understand their chemical reactivity in oxidation mechanisms in which this important molecule are involved.

2. RESULTS AND DISCUSSION

The oxidation mechanism of Betanidin (**Bd**) is highly affected by the medium pH.[17,18] Therefore, it is necessary to know the values of pK_a and the deprotonation positions of the **Bd** (Figure 1). In addition, it is generally assumed that the $^{+}N16H_2$ of **Bd** is deprotonated before the carboxylic acid groups.[10]

2.1. Conformational Analysis. The study began by calculating the energies of different conformations of fully protonated **Bd**. The most stable conformer was used to calculate the values of pK_a (Figure S1). This structure shows the presence of three intramolecular hydrogen bonds; one between the two hydroxyl groups attached to C5 and C6. The other two are formed by the oxygen atom from each carboxylic group in C15 and C17 with the hydrogen-bonded to N16; it is evidenced the dihedral angles between the donor and the receptor hydrogen bond groups are closed to 0° (Table S1). Similar optimized conformations were obtained with all basis sets used (Figure S2).

https://dx.doi.org/10.1021/acsomega.0c00904
ACS Omega XXXX, XXX, XXX−XXX

Table 1. pK_a Values Calculated Using Functional/Basis Set/SMD Implicit Model Level of Theory for First Deprotonation Sites of Betanidin

	6-31+G(d)			6-31+G(d,p)			6-31++G(d,p)			6-311+G(d,p)			6-311++G(d,p)		
	pK_aC2	pK_aC15	pK_aC17	pK_aC2	pK_aC15	pK_aC17	pK_aC2	pK_aC15	pK_aC17	pK_aC2	pK_aC15	pK_aC17	pK_aC2	pK_aC15	pK_aC17
B3LYP	0.34	0.38	−1.36	2.64	2.79	1.11	2.65	2.80	1.13	2.93	2.45	0.65	2.57	2.91	0.95
B3PW91	1.27	0.79	−1.33	3.20	3.56	1.79	3.87	3.27	1.19	3.80	3.19	1.33	3.83	3.16	1.61
PBE0	0.27	0.57	−1.44	3.33	2.73	0.94	3.44	3.07	1.20	2.97	3.07	1.10	2.98	3.11	1.39
ωB97XD	1.37	1.95	−1.11	3.58	3.89	1.32	3.60	3.89	1.35	4.05	3.32	0.86	4.11	3.39	1.16
M06-2X	−0.27	−0.04	−2.66	2.20	2.28	−0.18	2.65	2.02	0.12	2.25	1.51	−1.16	2.27	1.07	−0.69
fitting[a]															
B3LYP	2.11	2.35	1.57												
PBE0	2.12	2.26	1.30												
ωB97XD	2.64	2.39	1.02												
M06-2X	2.14	2.25	0.96												
M06-2X SAS[b]	2.71	2.73	0.93												
betanin[c]	1.5	3.4	3.4												

[a]Values obtained using reported fitting parameters (Galano et al.). [b]Values calculated modifying the SMD cavity surface (Lian, Johnston, Parks, and Smith). [c]Experimental estimated values for Betanin.

Next, the optimized **Bd** was deprotonated in each carboxylic group and optimized to obtain the lowest-energy structures for **BdC2**, **BdC15**, and **BdC17** (Figure 2). It is important to remark that the main structural parameters are preserved compared to the uncharged parental **Bd** molecule.

2.2. Calculation of Values of pK_a. *2.2.1. Effect of Calculation Methods in the Direct Approach.* To determine the best methodology to calculate values of pK_a, five DFT functionals (B3LYP, B3PW91, ωB97XD, PBE0, and M06-2X) and five basis sets (6-31+G(d), 6-31+G(d,p), 6-31++G(d,p), 6-311+G(d,p), and 6-311++G(d,p)) were used. These most stable conformers were used for the calculation of the values of pK_a. Experimental **Bd** pK_a values are unknown; these are the reasons to use the values of pK_a reported for betanin (**Bn**) as a reference. The pK_a for its phenolic OH group was measured to be 8.5; the pK_a of two carboxyl groups was suggested to be ∼3.4; the carboxyl group in the C2 position was suggested to have a lower pK_a due to the isoelectric point of betanin was found in the range of pH 1.5−2.0.[4,33]

When the calculations were performed using the 6-31+G(d) basis set, the values of pK_a were lower, even negative, compared with the reference values (Table 1). However, by including polarization functions on the H atom, 6-31+G(d,p), a remarkable effect of increased values of pK_a is observed. The pK_aC17 values are in the range of 0.94−1.79, and the values of pK_aC15 are between 2.45−3.89 and pK_aC2 2.64−4.11 (excluding all results obtained with 6-31+G(d) basis set and the M06-2X method). These results represent dispersion close to 1 pK_a unit between different functionals. On the other hand, pK_aC15 and pK_aC2 values do not show high differences if the comparison is made at the same theory level.

The diffuse functions are presumed to be critical in pK_a calculations, where are anions are involved. This is because charged species have a more spread out electron densities than neutral species, thus diffuse functions must be added to handle them adequately. Because, for the anionic species studied here, the negative charge is principally located on O atoms, using a diffuse function on nonhydrogen atoms is adequate to appropriately describe the molecules studied. This is proved by the fact that the results obtained with the basis sets 6-31++G(d,p), 6-311+G(d,p), and 6-311++G(d,p) are very similar, the values have the tendency to stabilize. However, the functional M06-2X seems to be the more susceptible electronic structure method, while for the other DFT methods this effect is minor. In this regard, it should be noted that the pK_a values strongly depend on the basis set size.

2.2.2. Exploration of Fitting and Scaled Solvent-Accessible Surface (SAS) Models. To obtain pK_a values using other different computational protocols, two general strategies were explored. These strategies correlate the experimental pK_a with free energy values obtained by theoretical calculations. In the first place, the reported empirical fitted equations ("Fitting model") for the calculation of carboxylic acids pK_a values were used (see Section 2.3).[31] The calculated pK_a values are reported in Table 1.

Recently, the pK_a calculation of carboxylic acids was reported using a scaled solvent-accessible surface and SMD solvation model (SMD_{SAS}).[32] This is the second protocol we have applied (Table 1).

The pK_aC17 values calculated are between 0.96 and 1.57 (fitting and SAS values; Table 1). With these methodologies, the pK_aC2 and pK_aC15 are very similar, 2.11−2.64 and 2.25−2.39, respectively. It is important to remark that these strategies were developed mainly with monoprotic acids.

In conclusion, the values of pK_a calculated with the B3LYP functional and mostly all basis set (6-31+G(d,p), 6-31++G(d,p), 6-311+G(d,p), and 6-311++G(d,p)) correlated better with the Fitting and SAS calculations. On the other hand, the values of pK_a calculated with the M06-2X level of theory were the most inaccurate values.

2.2.3. Electron Density and Electrostatic Potential Surface Analysis. The C17COOH group was found to first deprotonate at all levels of theory, similar to the observation of other authors.[34,35] This observation is contrary to the the pK_a value of approximately 1.5 reported for C2COOH group of betanin.[4] To understand this result, it is useful to analyze the electron density of the highest occupied molecular orbital (HOMO) and the electrostatic potential surface of **Bd** and its various deprotonated forms (Figure S3). The electron density of **Bd** is delocalized in the molecule's conjugate system (the DOPA ring and the conjugated double bonds that include C17). After proton removal, the electron density delocalizes toward the site of the missing proton, especially when the H of C2COOH or C15COOH is removed. It is beneficial to take

https://dx.doi.org/10.1021/acsomega.0c00904
ACS Omega XXXX, XXX, XXX−XXX

Table 2. Calculated pK_a Using Functional/6-31+G(d,p)/SMD and Explicit Water Molecules

	one water			three waters		
	pK_a-C2COOH	pK_a-C15COOH	pK_a-C17COOH	pK_a-C2COOH	pK_a-C15COOH	pK_a-C17COOH
B3LYP	2.97	2.51	1.51	1.26	1.00	0.84
B3PW91	3.86	3.44	2.10	3.14	1.67	1.11
PBE0	3.64	3.53	1.66	1.69	1.22	0.14
ωB97XD	4.89	4.43	2.12	1.67	1.13	0.92
M06-2X	2.48	2.90	0.62	0.11	1.06	0.07

Table 3. Calculated Values of pK_a for All Protic Groups

		pK_a1	pK_aC17C2[a]	pK_aC17C15[b]	pK_a3	pK_a4[c]	pK_a5[d]	pK_a6[e]
					SMD Model			
	6-31+G(d)	−1.36	1.17	0.99	1.38	9.40	17.55	21.99
	6-31+G(d,p)	1.11	2.93	3.38	5.71	10.59	19.97	23.99
B3LYP	6-31++G(d,p)	1.13	2.96	2.80	3.59	11.71	19.84	24.13
	6-311+G(d,p)	0.65	3.39	2.77	3.82	11.72	19.75	24.07
	6-311++G(d,p)	0.95	3.01	3.28	3.50	11.55	19.57	23.87
	6-31+G(d)	−1.33	2.31	1.70	2.64	9.88	18.21	23.77
	6-31+G(d,p)	1.79	4.09	4.20	4.64	12.15	20.74	25.81
B3PW91	6-31++G(d,p)	1.19	4.10	4.21	4.52	12.18	20.77	25.14
	6-311+G(d,p)	1.33	4.58	3.84	4.85	12.31	20.53	25.03
	6-311++G(d,p)	1.61	3.55	3.60	4.63	11.93	20.51	24.81
	6-31+G(d)	−1.44	1.05	1.24	1.88	9.18	17.64	23.48
	6-31+G(d,p)	0.94	4.09	3.31	4.44	11.88	19.79	24.93
PBE0	6-31++G(d,p)	1.20	3.46	3.72	4.53	11.58	20.28	25.17
	6-311+G(d,p)	1.10	3.50	3.73	6.18	8.78	16.98	25.01
	6-311++G(d,p)	1.39	3.28	3.49	4.57	11.55	20.25	25.04
	6-31+G(d)	−1.11	1.62	2.06	3.86	10.28	20.01	21.43
	6-31+G(d,p)	1.32	3.84	4.27	5.26	13.81	22.33	23.73
ωB97XD	6-31++G(d,p)	1.35	3.87	4.26	4.89	13.80	22.13	23.33
	6-311+G(d,p)	0.86	3.94	4.03	5.16	13.50	22.34	22.88
	6-311++G(d,p)	1.13	4.86	3.82	4.93	13.61	21.99	23.07
	6-31+G(d)	−2.66	0.62	1.29	1.14	9.62	17.75	18.94
	6-31+G(d,p)	−0.18	2.90	2.92	3.43	12.02	20.14	20.44
M06-2X	6-31++G(d,p)	0.12	3.03	2.02	3.40	12.07	20.18	20.45
	6-311+G(d,p)	−1.16	3.08	2.49	3.71	11.45	19.87	20.34
	6-311++G(d,p)	−0.69	2.68	2.06	3.33	11.35	19.50	20.49
					One Explicit Water[f]			
	B3LYP	1.51	3.48	3.27	4.24	10.80	15.95	16.66
	B3PW91	2.10	4.72	4.37	5.28	10.67	17.80	17.14
	PBE0	1.66	4.55	4.13	4.96	10.80	17.20	18.23
	ωB97XD	2.12	4.77	4.78	5.72	12.70	18.89	17.91
	M06-2X	0.62	2.96	3.47	3.76	10.68	17.93	13.94
					Fitting[g]			
	B3LYP	1.57	2.65		3.00	8.62	11.77	18.99
	PBE0	1.30	2.49		2.89	8.27	11.64	19.35
	ωB97XD	1.02		2.78	3.80	8.07	12.21	17.26
	M06-2X	0.96	2.49		2.83	8.46	11.96	17.88
	M06-2X SAS	0.93	3.43		4.10	11.31	18.94	18.93

[a]pK_aC17C2 = value for the second deprotonation in C2COOH. [b]pK_aC17C15 = value for the second deprotonation in C15COOH. [c]pK_a4 = deprotonation in C6OH. [d]pK_a5 = deprotonation in C5OH. [e]pK_a6 = deprotonation in N16H. [f]Basis set 6-31+G(d,p). [g]Parameters described in the Materials and Methods section.

away the C17COOH hydrogen because the electron density is slightly influenced after removing a proton.

2.2.4. Explicit Water Molecule Evaluation. Due to the good relation between computational cost, time consumption, and pK_a results expressed in Table 1, we decided to use 6-31+G(d,p) as a basis set to analyze the effects of explicit water molecules (Table 2).

The arrangement of one water molecule close to the protonation/deprotonation site improved the pK_a values over calculations without an explicit water molecule (Table 2). The effect observed in comparison with the results without water molecules is moderate; most pK_a values are shifted to lower values. Still, B3LYP/6-31+G(d,p) is a better approach. The SMD solvation model has some difficulties in accounting for the solvation of ions, just a single water molecule is capable of

https://dx.doi.org/10.1021/acsomega.0c00904
ACS Omega XXXX, XXX, XXX−XXX

Scheme 1. Proposed Acid−Base Behavior of Bd in Water

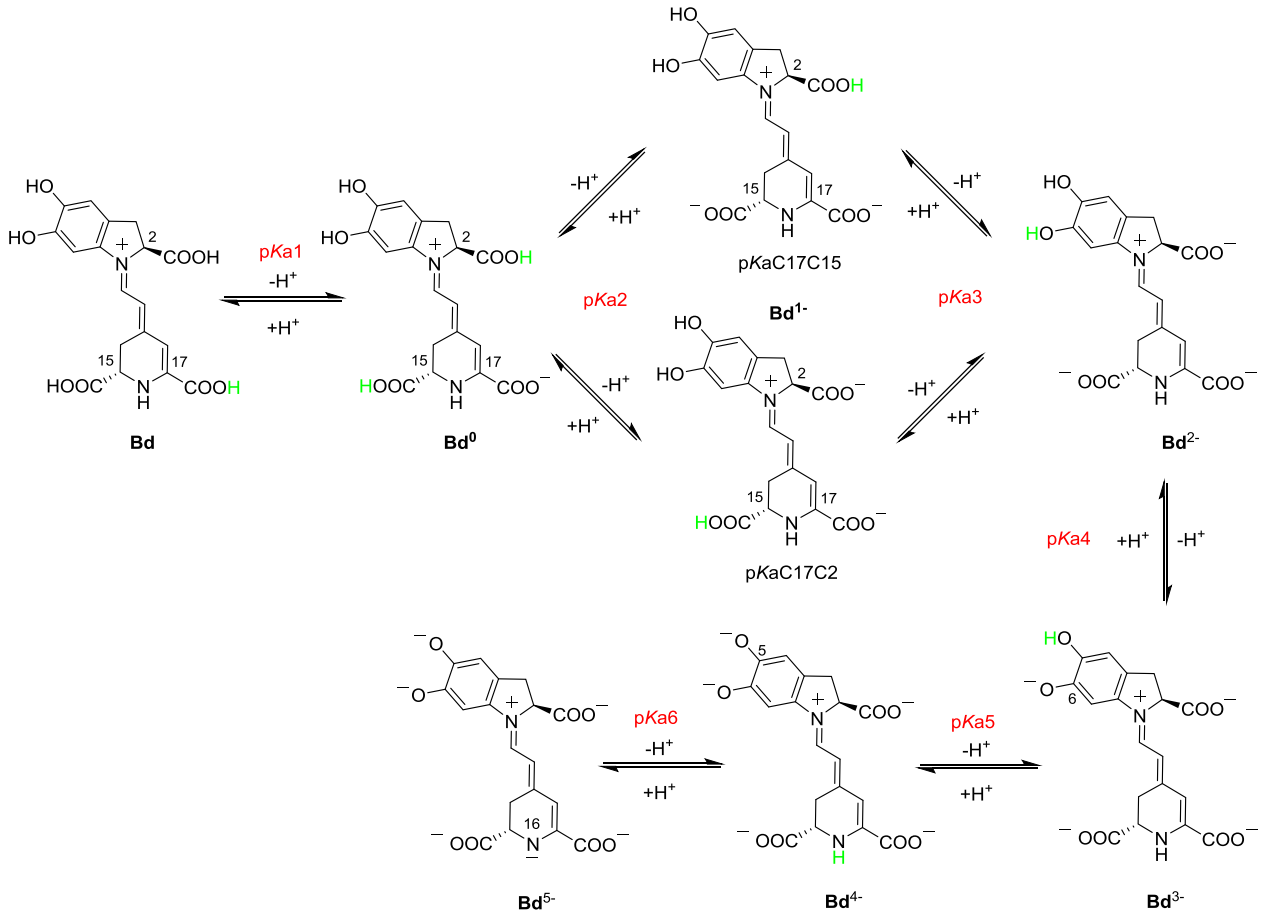

improving the pK_a values, and the influence is higher when the water is hydrogen-bonded to the deprotonation site. However, the addition of three water molecules produces an over-stabilization of ionic species, and all pK_a values decrease markedly moving away from the established reference values. Based on these results, we can postulate that in **Bd** first deprotonation occurs in the C17 carboxylic group.

2.3. Second and Subsequent Deprotonations. For evaluation, further deprotonations were performed following the same procedures except that only implicit SMD and explicit one water molecule models were used (Table 3). Once deprotonated, the C17COOH group calculations were not conclusive with respect to the second deprotonation of C2COOH (pK_aC17C2) or C15COOH (pK_aC17C15; Table 3 and Scheme 1).

The values obtained with Fitting and M06-2X$_{SAS}$ methods suggest that the second deprotonation occurs in C2COOH. The predicted pK_a values were between 2.49 and 2.78 in the fitting calculation; besides, a higher value of 3.43 was obtained by M06-2X$_{SAS}$. The main difference at this point is that M06-2X$_{SAS}$[32] was developed only with monoprotic species and Fitting calculation with few diprotic acids.[31]

On the other hand, when the pK_a values were computed using the direct approach with the SMD implicit model, some theories predict the second deprotonation in C2COOH and the others in C15COOH with values in the ranks of 2.68−4.86 and 2.92−4.93, respectively (Table 3). Once again, 6-31+G(d) basis set calculations yielded the worst results. Besides, four of the five functionals combined with 6-31+G(d,p) first predict the C2COOH deprotonation. On the contrary, when the basis sets were 6-31++G(d,p), 6-311+G(d,p), and 6-311++G(d,p), the C15COOH group was deprotonated second, with the exception of the PDBE0. The average pK_a value for C17C2 calculated without the 6-31+G(d) was 3.56 ± 0.60 (mean ± standard deviation (SD)) and that calculated for C17C15 using the implicit solvent model was 3.41 ± 0.70. However, calculations with one explicit water suggest that pK_aC17C2 and pK_aC17C15 are practically the same with each method used (Table 3). The average values are 4.10 ± 0.80 and 4.00 ± 0.60 for pK_aC17C2 and pK_aC17C15, respectively; the computational methodology cannot differentiate between them.

Finally, the third carboxylic deprotonation was studied to obtain pK_a3 values (Table 3 and Scheme 1). The fitting pK_a values were dispersed between 2.83−3.80, and M062-X$_{SAS}$ gives 4.1 pK_a units; at this point, the reference values are only guidance due mainly to the polyprotic nature of **Bd** that was not contemplated in these models as was mentioned previously. Also, all calculated pK_a3 values were in the rank of 3.33−5.71 (excluding PBE0/6311++G(d,p) value), approximately 1 unit bigger than the second pK_a values; the average value of the explicit approach was 4.8 ± 0.8. As a partial conclusion, we can propose the next deprotonation order pK_aC17 < pK_aC17C2 ≈ pK_aC17C15 < pK_a3 (Scheme 1).

On the other hand, the carboxylic deprotonations are followed by C6OH ionization (Scheme 1). In all calculations, the deprotonation order of the OH groups was C6OH first, followed by C5OH deprotonation (see Table S3 for one

https://dx.doi.org/10.1021/acsomega.0c00904
ACS Omega XXXX, XXX, XXX−XXX

example). The pK_a4 was estimated by the implicit SMD model at an average value of 11.5 ± 1.4, while this range is more precise in case one explicit water molecule is used, 10.7 ± 0.1, except that the ωB97XD values are always bigger. As expected, the SMD implicit model presents more inaccurate results due to the failure to solvate anionic and polyprotic species. A similar behavior was observed for pK_a5 and pK_a6 calculations, where the values present high discrepancies due to the complexity in reproducing correct solvation of ionic species. The SMD calculations suggest markedly that pK_a5 corresponds to C5OH deprotonation, followed by N16H deprotonation, having average values of 19.9 ± 1.5 and 23.3 ± 1.9, respectively; with one explicit water molecule, the values of 17.2 ± 0.9 and 16.5 ± 1.8 are almost the same. The pK_a values of monoprotic alcohols and amines calculated using only one explicit water molecule and SMD solvation are found to have average errors of 3 pK_a and 1 pK_a units, respectively.[29,32] Clearly, this background supports the results obtained in the hydroxyl and amine deprotonations. Finally, the pK_a values of C5OH and C6OH for **Bd** were obtained using B3LYP/6-311++G(d,p) and three explicit water molecules, as reported by Thapa and Schlegel.[29] The **Bd** C6OH deprotonation has a pK_a of 6.64, and the subsequent deprotonation of C5OH gives a pK_a of 11.20 (Table S3); these values are close to 8.5 assigned for C6OH for **Bn**.[4,33]

2.4. Carboxylic Acid Deprotonation Order. At this point, the more relevant issue of the present article is the prediction that the first deprotonation of **Bd** occurs in C17COOH, while it was postulated previously that this happens in the C2COOH group.[36] The isoelectric point of **Bn** was determined between 1.5 and 2.0;[36] the value of pK_a of the two less acidic carboxylic groups of **Bn** was 3.5;[4,33] both facts implying that the pK_a of the most acidic carboxylic group in **Bn** should be lower than 2.

On the other hand, **Bn** hydrolysis affords betalamic acid (**Bt**) and *cyclo*-DOPA-5-*O*-*β*-D-glucoside (Figure S4). The *cyclo*-DOPA-5-*O*-*β*-D-glucoside pK_a values were experimentally determined to be pK_aCOOH = 1.58, pK_aNH2 = 4.75, and pK_aOH6 = 9.42.[37] Recently, values of pK_a of **Bt** (unknown) were calculated using three theoretical methods (Marvin,[38,39] Jaguar,[40] and Epik[41]) in the range of 2.82−3.43 and 4.16−5.18 for the C10 and the C7, respectively; also, the pK_aC15COOH (2.96−4.0) and pK_aC17COOH (2.90−5.19) for **Bn** were calculated.[42] Moreover, the deprotonation of **Bn** C2COOH (pK_a = 1.5), C15COOH (pK_a = 3.7), C17COOH (pK_a = 3.0), OH6 (pK_a = 8.5), and N16H (pK_a = 10.3) were obtained using the Marvin method.[43]

Intending to unveil the mechanism of the first deprotonation of betalains (**Bn** and **Bd**), we decided to study the behavior of *cyclo*-DOPA-5-*O*-*β*-D-glucoside, **Bt**, and **Bn** by calculating the pK_a values for each molecule. For this purpose and based on the results presented here, a very good approach could be obtained using the B3LYP/6-31+G(d,p)/SMD with one explicit water model with a low computational cost. Following this approach, *cyclo*-DOPA-5-*O*-*β*-D-glucoside gave the values of pK_aCOOH = 1.39, pK_aNH2 = 4.52, and pK_aOH6 = 14.78 and **Bt** gave the values of pK_aC10COOH = 2.95 and pK_aC7COOH = 4.10; these results are in very good agreement with the above-described results. Furthermore, **Bn** showed the same behavior as **Bd** (Figure S5).

On the other hand, an exhaustive analysis of the reported ^{1}H NMR of **Bn** and **Bd** was made to unveil that the carboxylic group deprotonated first;[43−45] also, ^{1}H NMR was estimated for different deprotonation states of **Bd** using the DFT/SMD/B3LYP 6-31G+(d,p) methodology (Table S4). The H2 chemical shift (δ) of **Bn** at pH < 1 was reported to be 5.23 ppm, and a similar value was observed at pH 2.4. The H2 atom is more deshielded at pH 5 ($\Delta\delta$ of ca 0.29 ppm) due to the deprotonation of the carboxylic group attached to C2; a similar result was observed for **Bd** (Table S4). It is clear that C2COOH cannot be the carboxylic group of the first deprotonation. The effect of pH on other hydrogen atoms is less pronounced. In **Bn**, the H15 chemical shift cannot be assigned a lower pH due to the signal overlapping with deuterated water, but the δ at other pH values are similar. However, the **Bd** H15 presents a δ of 4.97 at a very acidic pH, but no experimental information is available at higher pH.

All these results support the fact that the methodology proposed for carboxylic acid pK_a determination is well-grounded and reliable and reproduces the experimental evidence. It is clear that the first deprotonation of **Bd** and **Bn** occurs in C17COOH, followed by C2COOH and C15COOH.

3. CONCLUSIONS

In the present article, we have developed a systematic study of **Bd** acid−base behavior using different theoretical approaches. In the first place, two models, Fitting and M06-2X$_{SAS}$, were used to have reference pK_a values because there is no experimental information. Further, the direct approach was used to compute the values of pK_a using a wide range of DFT methods with the SMD model, one and three explicit water molecules. The results show similar pK_a values for all methods using a more complex basis set of 6-31+G(d). Besides, we have shown that the inclusion of one explicit water molecule increases the accuracy of the calculated pK_a values mainly by improving the accuracy of the solvation free energies of the anions. The DFT B3LYP/631+G(d,p)/SMD with one water molecules allowed to analyze the system behavior quite well with a low computational cost. It is important to remark that **Bd** is a polyprotic molecule, whose experimental values of pK_a are still unknown, and systematic theoretical methods reported only allow the calculation of pK_a of monoanions and a few dianions. This study evaluated a key parameter, pK_a, which is needed to understand the structure and reactivity of **Bd** in solution.

4. MATERIALS AND METHODS

4.1. Computational Details. Calculations were performed by the Gaussian 09 revision E01 series of programs using five hybrid density functionals (B3LYP, B3PW91, ωB97XD, PBE0, and M06-2X), five basis sets (6-31+G(d), 6-31+G(d,p), 6-31++G(d,p), 6-311+G(d,p), and 6-311++G(d,p)), and the SMD implicit solvation model.[27,28] Geometries were fully optimized in aqueous solution. Harmonic frequencies were calculated to confirm that the structures were minima on the potential energy surface and to obtain the thermal and entropic contributions to the free energies. A conformational analysis was carried out considering all of the possible torsion angles of carboxylic and hydroxyl groups and the angles of C2N1C11H and C11C12C13C14 (Figure S1).

4.2. Direct Approach. The calculation of pK_a was based on the use of the direct approach, given by the proton dissociation reaction shown in eq 1.[24,29] The pK_a value of the molecule HA was calculated according to eq 2, where $G^*_{aq,A-}$

https://dx.doi.org/10.1021/acsomega.0c00904
ACS Omega XXXX, XXX, XXX−XXX

and $G^*_{aq,HA}$ are the standard free energies of the deprotonated and protonated species, respectively, calculated directly in aqueous solution at 298.15 K.

$$HA_{aq} \xrightarrow{\Delta G^*_{aq}} A^-_{aq} + H^+_{aq} \quad (1)$$

$$pK_a = \frac{\Delta G^*_{aq}}{2.303\,RT} = \frac{G^*_{aq,A^-} + G^*_{aq,H^+} - G^*_{aq,HA}}{2.303\,RT} \quad (2)$$

The Gibbs free energy of a proton in the aqueous phase is calculated using the following equations.[24,29]

$$G^*_{aq,H^+} = G^o_{g,H^+} + \Delta G^*_{aq,solv\,H^+} + \Delta G^{1\,atm\rightarrow 1\,M} \quad (3)$$

G^o_{g,H^+} = − 6.287 kcal/mol at 298 K.[29] $\Delta G^*_{aq,solv\,H^+}$ = −265.9 kcal/mol is the aqueous phase solvation free energy of the proton, taken from the literature.[30] $\Delta G^{1atm\rightarrow 1M} = RT\,(24.46)$ = 1.89 kcal/mol is a correction term for the change in a standard state of 1 atm to 1 mol/L. The symbols * and ° denote the standard state of 1 mol/L and 1 atm, respectively.

$$G^*_{aq,A^-} = E + \text{ZPVE} + (\text{electronic and thermal free energy correction})$$

$$G^*_{aq,HA} = E + \text{ZPVE} + (\text{electronic and thermal free energy correction})$$

where E is the electronic energy for A^- or HA obtained by structure optimization, ZPVE is the zero-point vibrational energy in solution. All pK_a calculations are given in the Supporting Information.

4.3. Fitting Model. The reported empirical fitted equations for the calculation of carboxylic acids pK_a values were used (eq 4).[31]

$$pK_a = m(G^*_{aq,A^-} - G^*_{aq,HA}) + C \quad (4)$$

The parameters "m" and "C" and the levels of theory used are listed in Galano et al. (see Table S2).[31] The Gibbs free energies were obtained as described in Section 4.2. In the Supporting Information, the calculations can be found.

4.4. Scaled Solvent-Accessible Surface (SAS) Model. The calculation is similar to that we presented for the M06-2X/6-31+G(d,p) level of theory in Section 4.2; the same equations were used. In the geometry optimizations, the surface type and the scaling factor options in the SCRF section were tuned. By choosing SAS as the solute−solvent boundary, the solvent radius (1.385 Å for water) is added to the intrinsic Coulomb radii to construct the cavity.[32] It is necessary to add the scale factor α = 0.485 and the surface of SAS in the input file (see an example in Supporting Information). No explicit water molecules were used.

4.5. Explicit Water Molecules Evaluation. To improve the calculation of the solvation effects that are important for pK_a calculations, mainly in charged structures, we included one and three explicit water molecules directly hydrogen-bonded to the site being protonated/deprotonated. For each hydrogen-bonding site, several orientations of the added water were considered and only the lowest-energy structure was used. For optimal cancellation of errors in pK_a calculations (as Section 4.2), the water molecule was hydrogen-bonded to the same site in the molecule and its deprotonated form. Typical arrangements of water near the protonation/deprotonation site are shown in Figure 3a,b.

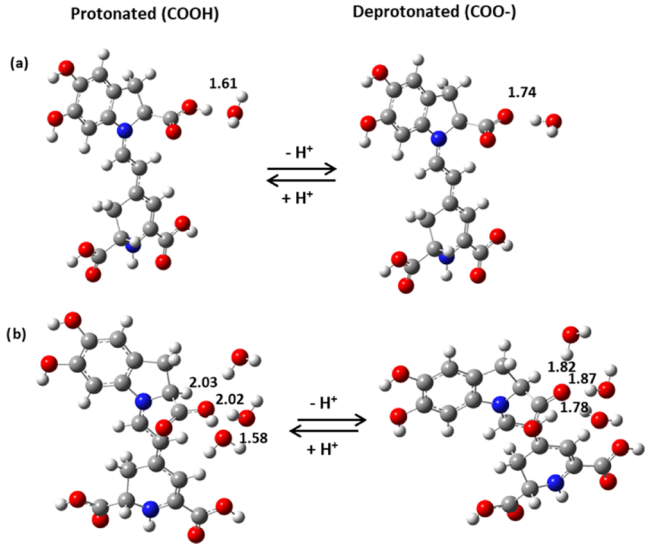

Figure 3. Arrangement of explicit water molecules near the COOH and COO^- groups: (a) one explicit water molecule and (b) three explicit water molecules. Some of the hydrogen bond lengths are shown (in Å).

For **Bd** with one explicit water molecule, the COOH group provides a H atom to form a hydrogen bond with the O of the water, whereas in the deprotonated form, the COO− forms a hydrogen bond with the H atom of the water molecule (Figure 3a). When there are three explicit water molecules near the COOH group, the O of one accepts the H from the COOH group and the other two donate H to form three hydrogen bonds. Besides, in the deprotonated form, COO− forms a hydrogen bond with one hydrogen atom from each of the three water molecules (Figure 3b). Similar conformations and the same number of hydrogen bonds in the parent molecules were kept as consistent as possible to avoid any bias that may result in unsystematic contributions to the calculated free energy. For the molecule having more than one stable conformer, the one with the lowest energy was used in the final calculations.

■ ASSOCIATED CONTENT

Supporting Information

The Supporting Information is available free of charge at https://pubs.acs.org/doi/10.1021/acsomega.0c00904.

Most stable conformation of **Bd**; structure parameters for the most stable conformation of **Bd** optimized at SMD/functional/6-31+G(d); optimized structures obtained for **Bd** with all computational methods; electron density (isovalue = 0.04) and electrostatic potential surface (isovalue = 0.02 density = 0.04. red = −0.1, blue = 0.65) of the HOMO of **Bd** and deprotonated forms calculated at DFT/B3LYP/6-31+G(d,p); the parameters "m" and "C" extracted from Galano et al., optimized with 6-31+G(d) basis set; C5OH and C6OH pK_a values obtained with SMD/B3LYP/6-311++G(d,p); computed and reported ^{1}H NMR of betanin and Betanidin; betanin hydrolysis products; **Bn** pK_avalues determined with B3LYP/6-31+G(d,p)/SMD with one explicit water

https://dx.doi.org/10.1021/acsomega.0c00904
ACS Omega XXXX, XXX, XXX−XXX

molecule; coordinates of the geometry optimized with SMD/B3LYP/6-31+G(d,p); geometries with one explicit water molecule optimized with SMD/B3LYP/6-31+G(d,p); geometries with three explicit water molecule optimized with SMD/B3LYP/6-31+G(d,p) in a docx document; and all calculated values of pK_a in an excel document. Example of SAS input file in a docx document (PDF)

Method (6-31+G(d,p)/SMD,3W) and method (B3LYP/6-311++G(d,p)/SMD,3W) (XLSX)

AUTHOR INFORMATION

Corresponding Author

Sergio A. Rodriguez − *CONICET, Instituto de Ciencias Químicas, FAyA, UNSE, Santiago del Estero 4200, Argentina;* orcid.org/0000-0002-0904-5817; Email: drsergiorod@gmail.com

Author

Maria T. Baumgartner − *INFIQC-Dpto. Química Orgánica, Fac. Ciencias Químicas, UNC, Ciudad Universitaria, Córdoba 5000, Argentina*

Complete contact information is available at: https://pubs.acs.org/10.1021/acsomega.0c00904

Notes

The authors declare no competing financial interest.

ACKNOWLEDGMENTS

The authors are grateful to Consejo Nacional de Investigaciones Cientificas y Técnicas (CONICET), FONCYT, SECYT UNSE, and SECYT UNC for funding. This work used computational resources from CCAD-UNC, which is part of SNCAD-MinCyT, Argentina.

REFERENCES

(1) Gandía-Herrero, F.; García-Carmona, F. Biosynthesis of Betalains: Yellow and Violet Plant Pigments. *Trends Plant Sci.* **2013**, *18*, 334−343.

(2) Delgado-Vargas, F.; Jiménez, A. R.; Paredes-López, O. Natural Pigments: Carotenoids, Anthocyanins, and Betalains - Characteristics, Biosynthesis, Processing, and Stability. *Crit. Rev. Food Sci. Nutr.* **2000**, *40*, 173−289.

(3) Bartoloni, F. H.; Gonçalves, L. C. P.; Rodrigues, A. C. B.; Dörr, F. A.; Pinto, E.; Bastos, E. L. Photophysics and Hydrolytic Stability of Betalains in Aqueous Trifluoroethanol. *Monatsh. Chem.* **2013**, *144*, 567−571.

(4) Nilsson, T. Studies into the Pigments in Beetroot (*Beta Vulgaris* L. Ssp. *Vulgaris* Var. *Rubra L.*). *Lantbrukshoegsk. Ann.* **1970**, *36*, 179−219.

(5) Strack, D.; Vogt, T.; Schliemann, W. Recent Advances in Betalain Research. *Phytochemistry* **2003**, 247−269.

(6) Herbach, K. M.; Stintzing, F. C.; Carle, R. Betalain Stability and Degradation - Structural and Chromatic Aspects. *J. Food Sci.* **2006**, *71*, R41−R50.

(7) Georgiev, V. G.; Weber, J.; Kneschke, E.-M.; Denev, P. N.; Bley, T.; Pavlov, A. I. Antioxidant Activity and Phenolic Content of Betalain Extracts from Intact Plants and Hairy Root Cultures of the Red Beetroot Beta Vulgaris Cv. Detroit Dark Red. *Plant Foods Hum. Nutr.* **2010**, *65*, 105−111.

(8) Esatbeyoglu, T.; Wagner, A. E.; Schini-Kerth, V. B.; Rimbach, G. Betanin-A Food Colorant with Biological Activity. *Mol. Nutr. Food Res.* **2015**, *59*, 36−47.

(9) Vidal, P. J.; López-Nicolás, J. M.; Gandía-Herrero, F.; García-Carmona, F. Inactivation of Lipoxygenase and Cyclooxygenase by Natural Betalains and Semi-Synthetic Analogues. *Food Chem.* **2014**, *154*, 246−254.

(10) Gandía-Herrero, F.; Escribano, J.; García-Carmona, F. Structural Implications on Color, Fluorescence, and Antiradical Activity in Betalains. *Planta* **2010**, *232*, 449−460.

(11) Gandía-Herrero, F.; Escribano, J.; García-Carmona, F. The Role of Phenolic Hydroxy Groups in the Free Radical Scavenging Activity of Betalains. *J. Nat. Prod.* **2009**, *72*, 1142−1146.

(12) Gaertner, V. L.; Goldman, I. L. Pigment Distribution and Total Dissolved Solids of Selected Cycles of Table Beet from a Recurrent Selection Program for Increased Pigment. *J. Am. Soc. Hortic. Sci.* **2005**, *130*, 424−433.

(13) Attoe, E. L.; Von Elbe, J. H. Photochemial Degradation of Betanine and Selected Anthocyanins. *J. Food Sci.* **1981**, *46*, 1934−1937.

(14) Skopińska, A.; Tuwalska, D.; Wybraniec, S.; Starzak, K.; Mitka, K.; Kowalski, P.; Szaleniec, M. Spectrophotometric Study on Betanin Photodegradation. *Challenges Mod. Technol.* **2012**, *3*, 34−38.

(15) Gandía-Herrero, F.; Escribano, J.; García-Carmona, F. Characterization of the Activity of Tyrosinase on Betanidin. *J. Agric. Food Chem.* **2007**, *55*, 1546−1551.

(16) Martínez-Parra, J.; Muñoz, R. Characterization of Betacyanin Oxidation Catalyzed by a Peroxidase from *Beta Vulgaris* L. Roots. *J. Agric. Food Chem.* **2001**, *49*, 4064−4068.

(17) Wybraniec, S.; Michalowski, T. New Pathways of Betanidin and Betanin Enzymatic Oxidation. *J. Agric. Food Chem.* **2011**, *59*, 9612−9622.

(18) Ho, J.; Ertem, M. Z. Calculating Free Energy Changes in Continuum Solvation Models. *J. Phys. Chem. B* **2016**, *120*, 1319−1329.

(19) Wybraniec, S.; Starzak, K.; Skopińska, A.; Nemzer, B.; Pietrzkowski, Z.; Michałowski, T. Studies on Nonenzymatic Oxidation Mechanisms in Neobetanin, Betanin, and Decarboxylated Betanins. *J. Agric. Food Chem.* **2013**, *61*, 6465−6476.

(20) Kumorkiewicz, A.; Szmyr, N.; Popenda, Ł.; Pietrzkowski, Z.; Wybraniec, S. Alternative Mechanisms of Betacyanin Oxidation by Complexation and Radical Generation. *J. Agric. Food Chem.* **2019**, *67*, 7455−7465.

(21) Knorr, F. J.; McHale, J. L.; Clark, A. E.; Marchioro, A.; Moser, J.-E. Dynamics of Interfacial Electron Transfer from Betanin to Nanocrystalline TiO2: The Pursuit of Two-Electron Injection. *J. Phys. Chem. C* **2015**, *119*, 19030−19041.

(22) Wendel, M.; Nizinski, S.; Tuwalska, D.; Starzak, K.; Szot, D.; Prukala, D.; Sikorski, M.; Wybraniec, S.; Burdzinski, G. Time-Resolved Spectroscopy of the Singlet Excited State of Betanin in Aqueous and Alcoholic Solutions. *Phys. Chem. Chem. Phys.* **2015**, *17*, 18152−18158.

(23) Ho, J.; Ertem, M. Z. Calculating Free Energy Changes in Continuum Solvation Models. *J. Phys. Chem. B* **2016**, *120*, 1319−1329.

(24) Ho, J. Are Thermodynamic Cycles Necessary for Continuum Solvent Calculation of PKas and Reduction Potentials? *Phys. Chem. Chem. Phys.* **2015**, *17*, 2859−2868.

(25) Ho, J.; Coote, M. L. A Universal Approach for Continuum Solvent PKa Calculations: Are We There Yet? *Theor. Chem. Acc.* **2010**, *125*, 3−21.

(26) Marenich, A. V.; Ding, W.; Cramer, C. J.; Truhlar, D. G. Resolution of a Challenge for Solvation Modeling: Calculation of Dicarboxylic Acid Dissociation Constants Using Mixed Discrete-Continuum Solvation Models. *J. Phys. Chem. Lett.* **2012**, *3*, 1437−1442.

(27) Frisch, M. J.; Trucks, G. W.; Schlegel, B. H.; Scuseria, E. G.; Robb, A. M.; Cheeseman, J. R.; Scalmani, G.; Barone, V.; Mennucci, B.; Petersson, G. A.; Nakatsuji, H.; Caricato, M.; Li, X.; Hratchian, P. H.; Izmaylov, F. A.; Bloino, J.; Zheng, G.; Sonnenberg, L. J.; Frisch, M. J.; Trucks, W. G.; Schlegel, B. H.; Scuseria, E. G.; Robb, A. M.; C, G. J. R.; Scalmani; Barone, V.; Mennucci, B.; H; P, G. A.; Nakatsuji; Caricato, M.; Li, X.; Hratchian, P. H.; Izmaylov, F. A.; Bloino, J.; Zheng, G.; Sonnenberg, L. J.; M. H, K.; E, M.; Toyota; Fukuda, R.;

Hasegawa, J.; Ishida, M.; Nakajima, T.; Honda, Y.; Kitao, O.; Nakai, H.; Vreven, T.; M, E. J., Jr.; Peralta, J. A.; Ogliaro, F.; Bearpark, M.; Heyd, J. J.; Brothers, E.; Kudin, N. K.; R. V. N, S.; Kobayashi; N, K. J.; Raghavachari; Rendell, A.; Burant, C. J.; Iyengar, S. S.; Tomasi, J.; Cossi, M.; Rega, N.; Millam, M. J.; Klene, M.; Knox, E. J.; Cross, B. J.; Bakken, V.; Adamo, C.; Jaramillo, J.; Gomperts, R.; Stratmann, E. R.; Yazyev, O.; Austin, J. A.; Cammi, R.; Pomelli, C.; Ochterski, W. J.; Martin, L. R.; Morokuma, K.; Zakrzewski, G. V.; Voth, A. G.; Salvador, P.; D, S. J. J.; Dapprich; Daniels, D. A.; Farkas, Ö.; Foresman, B. J.; Ortiz, V. J.; Cioslowski, J.; Fox, D. J. [Oxygen Affinity of Haemoglobin (Author's Transl)]. *Bull. Physiopathol. Respir. (Nancy).* **2009**, *11*, 79−170.

(28) Marenich, A. V.; Cramer, C. J.; Truhlar, D. G. Performance of SM6, SM8, and SMD on the SAMPL1 Test Set for the Prediction of Small-Molecule Solvation Free Energies. *J. Phys. Chem. B* **2009**, *113*, 4538−4543.

(29) Thapa, B.; Schlegel, H. B. Improved PKa Prediction of Substituted Alcohols, Phenols, and Hydroperoxides in Aqueous Medium Using Density Functional Theory and a Cluster-Continuum Solvation Model. *J. Phys. Chem. A* **2017**, *121*, 4698−4706.

(30) Isse, A. A.; Gennaro, A. Absolute Potential of the Standard Hydrogen Electrode and the Problem of Interconversion of Potentials in Different Solvents. *J. Phys. Chem. B* **2010**, *114*, 7894−7899.

(31) Galano, A.; Pérez-González, A.; Castañeda-Arriaga, R.; Muñoz-Rugeles, L.; Mendoza-Sarmiento, G.; Romero-Silva, A.; Ibarra-Escutia, A.; Rebollar-Zepeda, A. M.; León-Carmona, J. R.; Hernández-Olivares, M. A.; Alvarez-Idaboy, J. R. Empirically Fitted Parameters for Calculating PKa Values with Small Deviations from Experiments Using a Simple Computational Strategy. *J. Chem. Inf. Model.* **2016**, *56*, 1714−1724.

(32) Lian, P.; Johnston, R. C.; Parks, J. M.; Smith, J. C. Quantum Chemical Calculation of p Kas of Environmentally Relevant Functional Groups: Carboxylic Acids, Amines, and Thiols in Aqueous Solution. *J. Phys. Chem. A* **2018**, *122*, 4366−4374.

(33) Zabihi, F.; Kiani, F.; Yaghobi, M.; Shahidi, S. A. The Theoretical Calculations and Experimental Measurements of Acid Dissociation Constants and Thermodynamic Properties of Betanin in Aqueous Solutions at Different Temperatures. *J. Solution Chem.* **2019**, *48*, 1438−1460.

(34) Qin, C.; Clark, A. E. DFT Characterization of the Optical and Redox Properties of Natural Pigments Relevant to Dye-Sensitized Solar Cells. *Chem. Phys. Lett.* **2007**, *438*, 26−30.

(35) Oprea, C. I.; Dumbrava, A.; Enache, I.; Georgescu, A.; Gîrţu, M. A. A Combined Experimental and Theoretical Study of Natural Betalain Pigments Used in Dye-Sensitized Solar Cells. *J. Photochem. Photobiol., A* **2012**, *240*, 5−13.

(36) Reznik, H. Die Pigmente Der Centrospermen Als Systematisches Element - II. Untersuchungen Über Das Ionophoretische Verhalten. *Planta* **1957**, *49*, 406−434.

(37) Wyler, H.; Meuer, U.; Bauer, J.; Stravs-Mombelli, L. Cyclodopa Glucoside (= (2S)-5-(B-D-glocopyranosyloxy)-6-hydroxyindoline-2-carboxylic Acid) and Its Occurrence in Red Beet (*Beta Vulgaris* Var. *Rubra* L.). *Helv. Chim. Acta* **1984**, *67*, 1348−1355.

(38) Szegezdi, J.; Csizmadia, F. In *A Method for Calculating the PK Values of Small and Large Molecules*, ACS National Meeting, 2007; pp 1−2.

(39) Szegezdi, J.; Csizmadia, F. In *Prediction of Dissociation Constant Using Microconstants*, ACS National Meeting, 2004; pp 2−3.

(40) Bochevarov, A. D.; Harder, E.; Hughes, T. F.; Greenwood, J. R.; Braden, D. A.; Philipp, D. M.; Rinaldo, D.; Halls, M. D.; Zhang, J.; Friesner, R. A. Jaguar: A High-Performance Quantum Chemistry Software Program with Strengths in Life and Materials Sciences. *Int. J. Quantum Chem.* **2013**, *113*, 2110−2142.

(41) Shelley, J. C.; Cholleti, A.; Frye, L. L.; Greenwood, J. R.; Timlin, M. R.; Uchimaya, M. Epik: A Software Program for PKa Prediction and Protonation State Generation for Drug-like Molecules. *J. Comput.-Aided Mol. Des.* **2007**, *21*, 681−691.

(42) Tutone, M.; Lauria, A.; Almerico, A. M. Theoretical Determination of the PK a Values of Betalamic Acid Related to the Free Radical Scavenger Capacity: Comparison Between Empirical and Quantum Chemical Methods. *Interdiscip. Sci.: Comput. Life Sci.* **2016**, *8*, 177−185.

(43) Esteves, L. C.; Pinheiro, A. C.; Pioli, R. M.; Penna, T. C.; Baader, W. J.; Correra, T. C.; Bastos, E. L. Revisiting the Mechanism of Hydrolysis of Betanin. *Photochem. Photobiol.* **2018**, *94*, 853−864.

(44) Stintzing, F. C.; Conrad, J.; Klaiber, I.; Beifuss, U.; Carle, R. Structural Investigations on Betacyanin Pigments by LC NMR and 2D NMR Spectroscopy. *Phytochemistry* **2004**, *65*, 415−422.

(45) Wyler, H.; Dreiding, A. S. Deuterierung von Betanidin Und Indicaxanthin, (E/Z)-Stereoisomerie in Betalainen. *Helv. Chim. Acta* **1984**, *67*, 1793−1800.

https://dx.doi.org/10.1021/acsomega.0c00904
ACS Omega XXXX, XXX, XXX−XXX